Experiments and Computations on the Compression Process in the Free Piston Shock Tunnel FD21

Bi Zhixian[1]*, Zhang Bingbing[1], Zhu Hao[1], Chen Xing[1],

Shen Junmou[1], Li Chen[1], Sun Riming[1]

[1] China Academy of Aerospace Aerodynamics, Beijing, China

*zbbfree@163.com

Abstract

The assembly of a new free piston shock tunnel facility FD21 at China Academy of Aerospace Aerodynamics (CAAA) is almost finished in 2017. Preliminary results on the compression process of driver gas by a free piston which is studied experimentally and numerically are presented. Initially the facility is operated at very low enthalpy level to avoid severe facility damage. Piston motion and pressure distributions at the end of compression tube, with the end of the compression tube closed, and with the diaphragm bursting, are compared with calculated values in the cases of air and He-Ar mixture as driver gases. Test results indicate that a soft piston landing is achieved on condition that the parameters reservoir air pressure, compression tube filling pressure and driver gas mixture were chosen properly. The numerical tools used are the analysis method by Hornung.

1 Introduction

In order to duplicate the high temperature real gas flow encountered by atmospheric reentry flight of space vehicles in ground testing, we have to ensure that the energy of the stream produced must match that in flight. This demand can be realized by a free piston shock tunnel which can generate high enthalpy, high density flows. Facilities of this type were proposed by Stalker in 1960's and have been successfully operating in a number of different institutions worldwide for many years, such as T4 at the University of Queensland in Australia, T5 at the California Institute of Technology in the United States, HEG at the German Aerospace Center (DLR) and HIEST at the Japan Aerospace Exploration Agency (JAXA). For the recent two decades, the range of operating conditions of these facilities has been extended for the investigation of scramjet engines.

Free piston shock tunnels consist of high-pressure air reservoir, compression tube, shock tube, nozzle, test section and vacuum tank. The compression tube and the shock tube are separated via the primary diaphragm and filled with a driver gas and a driven gas, respectively. Helium or mixture of helium and argon are typically used as the driver gas and air is used as the driven gas. The high pressure air stored in the high-pressure air reservoir is utilized to accelerate a heavy piston down the compression tube. The driver gas is compressed with the piston until the main diaphragm rupture. Then, the primary shock wave is generated and travels through the shock tube and the stagnation condition of the test gas is made after the shock reflection at the shock tube end. This gas then begins to flow through the hypersonic nozzle and generates a hypervelocity flow in the test section. The above working principle of free piston shock tunnel shows that the control of the piston motion is crucial to the performance of the shock tunnel and facility safety. The biggest disadvantage of this high enthalpy facility is short flow duration, with the test time of

approximately 5 ms or less. Tuned piston operation and tailored interface mode were proposed to increase the duration. In tuned operation, piston need land soft and the pressure at the end of compression tube after diaphragm rupture must be held almost constant for a certain time period. To realize the operation, it is required to choose proper parameters such as reservoir air pressure, compression tube filling pressure, driver gas mixture, diaphragm burst pressure and piston mass .etc.

A new large-sized free piston shock tunnel FD21 was built by China Academy of Aerospace Aerodynamics during 2014~2017. This paper presents the new results of calibration of FD21. The compression process of driver gas by a free piston is studied experimentally and numerically. The code used for the calculation of piston motion is based on a parametric analysis by Hornung.

2 The Free Piston Shock Tunnel FD21

The free piston shock tunnel FD21 is operated as a reflected type shock tunnel. A schematic overview of the facility is shown in figure 1. Identical with any free piston shock tunnel in existence, the FD21 facility consists of high-pressure air reservoir, compression tube, main diaphragm station, shock tube, nozzle, test section and vacuum tank. The high-pressure air reservoir can sustain up to 20MPa gas pressure and has a volume of 24m3.The compression tube has a length of 75m and a diameter of 0.668m. The shock tube is 34m long with a diameter of 0.29m. The nozzle exit diameter is max. 2000mm. The whole assembly can move freely in axial direction during operation of the free piston driver.

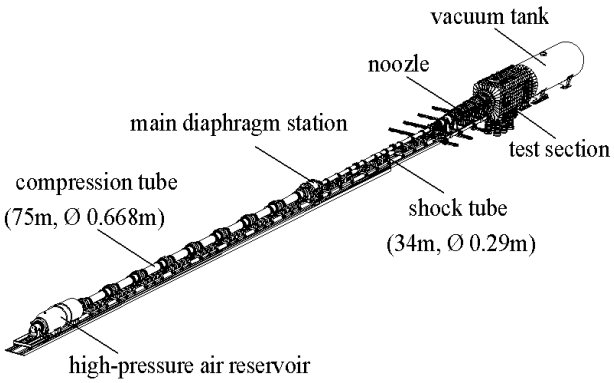

Figure 1 Schematic view of the free piston shock tunnel FD21

The facility is designed to achieve a total specific enthalpies in the range of 5~28MJ/kg, and the flow velocity 3~7km/s. Subsequently, the total enthalpy conditions range will be extended, higher for the investigation of re-entry configurations and lower for scramjet flight experiment configurations. It is planned to use several piston weights, ranges from 120~600kg, to generate different operating conditions. For the initial operation, pistons of two different weights are available at present, the light one is 124kg and the heavy one is 205kg. Piston buffers are mounted at the end of compression tube to absorb the remaining kinetic energy of the piston.

3 Experimental Setup and Numerical Model

As shown in figure 2, there are 8 piston register photoelectric sensors (E1~E8) installed in the side walls of the compression tube, along with 9 pressure sensors (C1~C9). Thus the piston trajectory as a function of position and time could be measured relatively accurately with 8 photoelectric sensors distributed along the compression tube. Pressure sensors are utilized to monitor the propagation and reflection of the compression waves owing to the piston motion. Nine shock register piezoelectricity pressure sensors

(S1~S9) are installed in the side walls of shock tube to monitor the shock velocity. One sensor S10 is installed in the end wall to measure the incident shock velocity and the pressure rise caused by the reflection of the incident shock wave.

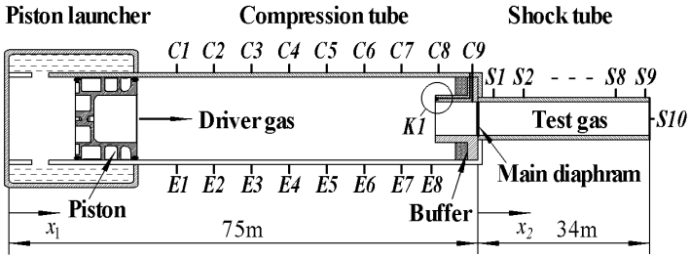

Figure 2 Position of the sensors along compression tube and shock tube (C1~C9: strain pressure sensors, E1~E8: photoelectric sensors, S1~S10: piezoelectric pressure sensors, K1: laser distance measuring sensor), and the piston motion measurement system.

The prediction approach of piston motion is described by Hornung. Quasi-one-dimensional flows are assumed in the numerical model. The piston motion is described by the following equations of motion. Equation 1 describes the piston motion before diaphragm burst; equation 2 describes the piston motion after diaphragm burst. The nonlinear equation is solved using the Runge-Kutta method.

$$-M_p \frac{d^2x}{dt} = \frac{\pi D^2}{4}\left[P_{A,0}\left(1 - \frac{\gamma_A - 1}{2}\frac{u_p}{a_{A,0}}\right)^{\frac{2\gamma_A}{\gamma_A - 1}} - P_{dr,0}\left(\frac{x}{L}\right)^{-\gamma_{dr}} \right] \tag{1}$$

$$-M_p \frac{d^2x}{dt} = \frac{\pi D^2}{4} P_{A,0}\left[\frac{P_{A,r}}{P_{A,0}} - \frac{P_{dr,r}}{P_{A,0}}\left(\frac{m_{dr}}{m_{dr,r}}\frac{x_r}{x}\right)^{\gamma_{dr}} \right] \tag{2}$$

Table 1 Test cases for the FD21 facility

case	Mp*(kg)	$P_{A,0}$(MPa)	$P_{dr,0}$(kPa)	$P_{dn,0}$(kPa)	Driver gas
24	124	0.8	25	——	air
32	205	0.8	25.7	100	air
36	205	0.8	20	100	5%He+95%Ar

4 Results and Discussion

To avoid severe damage in the larger-sized facility, the calibration of the free piston shock tunnel is started from low enthalpy level at present. The free piston driver is studied with the end of the compression tube closed, and with the diaphragm bursting in the cases of air and He-Ar mixture as driver gases. Table 1 gives an overview on the piston parameters for some test cases will be used in the following text.

Integrated efficiency of the free piston driver, which is decided mainly by the efficiency of piston launcher, the leak of driver gas between piston and the compression tube, and friction losses, is a significant parameter used for revising the numerical model with actual behavior of the piston compressor. A series of piston experiments are implemented with the end of the compression tube closed for the purpose of acquiring the integrated efficiency. Figure 3 gives the pressure history at the compression tube end and piston velocity vs. position of a typical test case 24#. In this test, the end of compression tube is

enveloped with a mental plate and the mass of piston is 124kg with air as driver gas. The piston has passed through the position of sensor C7(x=71.89m) which can be learnt from the signals of C7 and E7. The piston reversal starts at the position of 72.3m and then moves back and forth between sensor E3 and E7. The peak velocity of piston reaches up to 260m/s and the peak pressure at the end of compression tube reaches up to 6MPa, while strong pressure oscillations have been observed at the station just before the metal plate. The pressure in front of the piston, builds up in successive steps, due to compression waves generated by the piston motion, which undergo back-and-forth reflections at the end of compression tube and the piston front face. In fact, the amplitude of pressure oscillations decreases for a heavy piston under the same initial conditions. However, the pressure rise should be as smooth as possible, to avoid breaking the diaphragm at a pressure level differing from the design value. Eventually, the 205kg piston is chose to carry on the following piston compressor tests. After a number of tests with the end of the compression tube closed, integrated efficiency of the free piston driver falls in the range of 0.65~0.74. Anyway, good agreements between experiments with calculations have made it possible to carry on the following diaphragm tests.

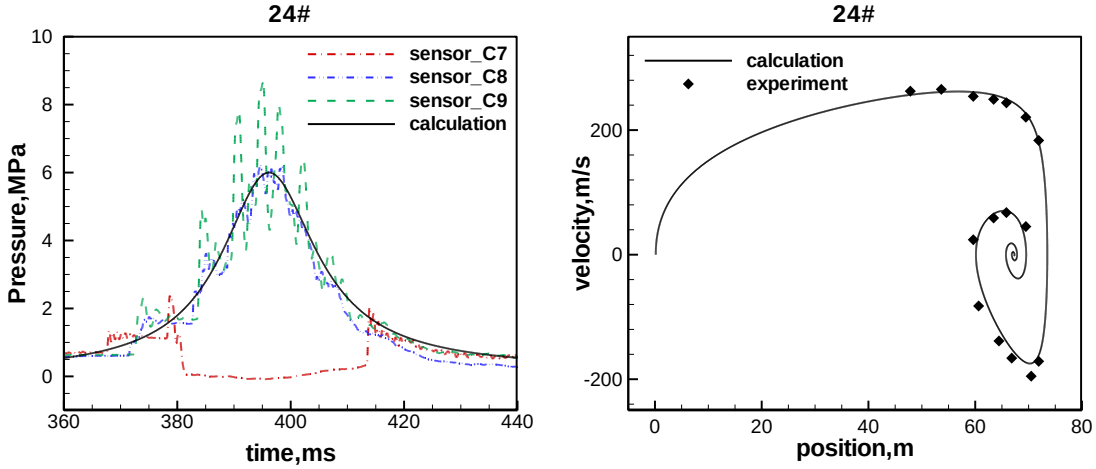

Figure 3 Pressure history at the compression tube end and Piston velocity vs. position for the 124kg piston

Figure 4 and figure 5 show the results of the comparison with theoretical prediction for two different driver gases: air and mixture of helium and argon. The most important part of the piston behavior is the motion after main diaphragm rupture, which cannot be resolved with the photoelectric sensors mounted on the compression tube wall. This part of piston motion is determined with the help of the laser distance measuring sensor, this part of experiments will be conducted and the results will be published soon. It shows that a good agreement is obtained between the predicted piston velocity and the experiment over the total length of the compression tube. The peak velocity of piston reaches 201 m/s in test case 32#, and 205m/s for case 36#. In order to achieve tuned piston operation, the piston must come to rest before reaching the buffer at the end of the compression. It can be seen in the two figures, the piston reversal starts before the buffer.

Figure 5 shows the pressure distributions along the compression tube and at the end of compression tube for the two different driver gases with the burst pressure of 3.5 MPa. The maximum pressure reaches 4.7MPa in case 32#, and 4MPa in case 36#. After main diaphragm rupture, the holding time of constant values is 14ms in case 32#, and 8ms in case 36#.

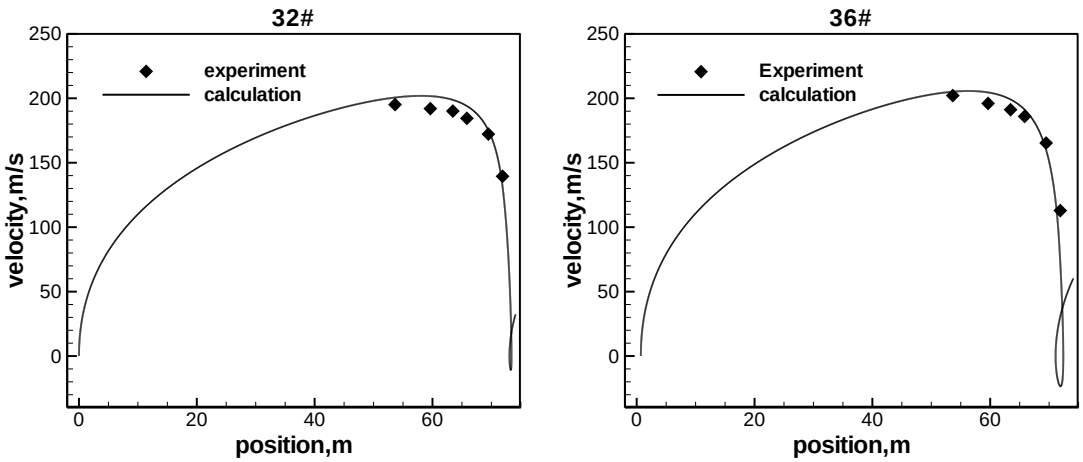

Figure 4 Piston velocity vs. position for the 205kg piston (test cases 32# and 36#)

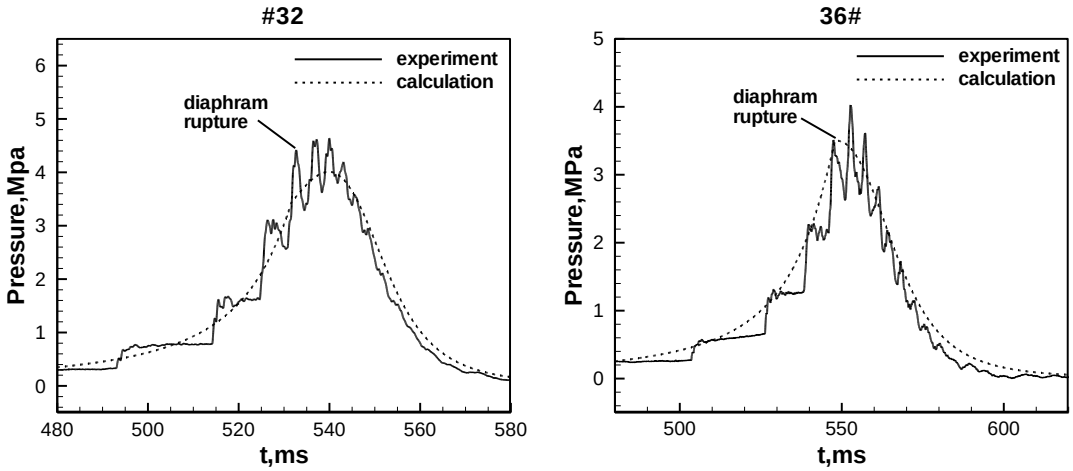

Figure 5 Pressure history at the end of compression tube (test cases 32# and 36#)

Figure 6 presents the pressure trace at the end of shock tube. From sensor S9, the first pressure step denotes that the incident shock wave is initiated and propagates along the shock tube, and the second pressure step denotes that the shock wave reaches the end of shock tube and reflects back, thus compressing the test gas for a second time. After shock reflection, the pressure level at the end of shock tube should be maintained for a certain time. A nozzle reservoir pressure of 4MPa can be reached for both cases. The holding time reaches up to 4ms in case 32# and 1-2ms in case 36#.

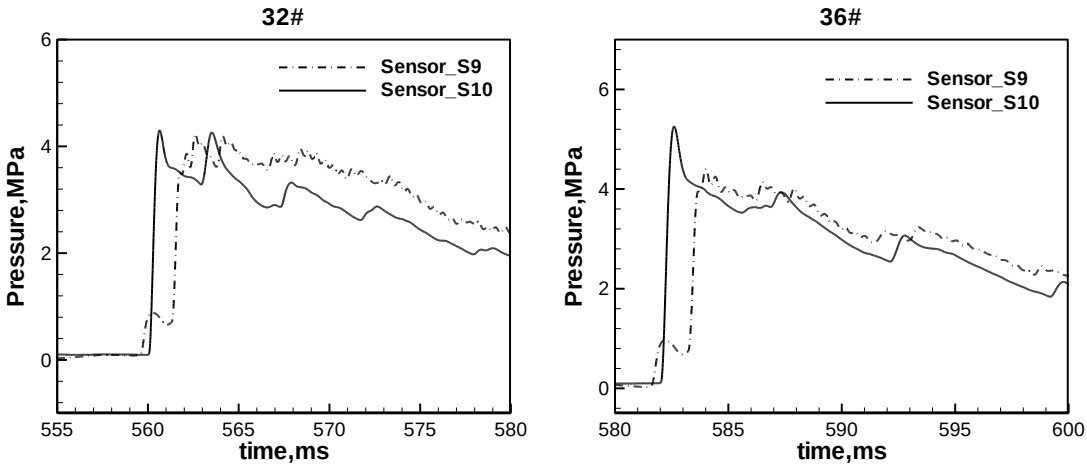

Figure 6 Pressure history at the end of shock tube

References

Stalker, R.J. (1967), "A study of the free-piston shock tunnel", *AIAA Journal* Vol. 5 No. 12, 1967, pp. 2160-2165.

Stalker, R.J. (1972), "Development of a Hypervelocity wind tunnel", *The Aeronautical Journal*, Vol. 36, 1972, pp. 374-384.

Gai, S.L. (1992), "Free piston shock tunnels: developments and capabilities", *Prog. Aerospace Sci.* Vol.29, 1992, 1-41.

Hornung, H.G. (1988), "The piston motion in a free-piston driver for shock tubes and tunnels", *GALCIT Rept.* FM 88-1, 1988

Hornung, H.G. (1992), "Performance data of the new free-piston shock tunnel at GAL CIT", *AIAA* 92-3943, 1992.

Hornung, H., Bélanger, J. (1990), "Role and Techniques of Ground Testing for Simulation of Flows up to Orbital Speed", *AIAA*-90-1377, 1990.

Eitellberg, G., McIntyre, T. J. Beck, W.H., Lacey, J. (1992), "The high enthalpy shock tunnel in Gottingen", *AIAA* -92-3942, 1992.

Eitellberg, G. (1994), "First results of calibration and use of HEG", *AIAA*-94-2525, 1994.

Itoh, K. (2000), "Characteristics of the HIEST and its applicability for hypersonic aero-thermodynamic and scramjet research", *Advanced hypersonic test facilities*, Chapter 8, 123-155, 2000.

Jacobs, P. A. (1994) "Quasi-one-dimensional modeling of free piston shock tunnel", *AIAA Journal*, Vol.32, No.1, 137-145. 1994.